



Research paper

Reconstruction of 3D Stack of Stars in Cardiac MRI using a Combination of GRASP and TV

Mitra Tavakkoli¹, Ataollah ebrahimzadeh¹, Abbas Nasiraei Moghaddam² and Javad Kazemitabar^{1*}

1. Electrical and Computer Engineering, Babol Noshirvani University of Technology, Babol, Mazandaran, Iran.

2. Biomedical Engineering, Amirkabir University of Technology (Tehran Polytechnic), Tehran, Iran.

Article Info

Article History:

Received 06 November 2020

Revised 25 June 2021

Accepted 05 September 2021

DOI:10.22044/JADM.2021.10232.2161

Keywords:

Cardiac MRI, Golden Ratio Radial Acquisition, Compressive Sensing.

*Corresponding author:
j.kazemitabar@nit.ac.ir (J. Kazemitabar).

Abstract

One of the most advanced non-invasive medical imaging methods is MRI that can make a good contrast between soft tissues. The main problem with this method is the time limitation in data acquisition, particularly in dynamic imaging. Radial sampling is an alternative for a faster data acquisition, and has several advantages compared to the Cartesian sampling. Among them, robustness to motion artifacts makes this acquisition useful in cardiac imaging. Recently, CS has been used in order to accelerate data acquisition in dynamic MRI. Cartesian acquisition uses irregular under-sampling patterns to create incoherent artifacts to meet the incoherent sampling requirement of CS. Radial acquisition, due to its incoherent artifact, even in regular sampling, has an inherent fitness to CS reconstruction. In this work, we reconstruct the (3D) stack of stars data in cardiac imaging using a combination of the TV penalty function and the GRASP algorithm. We reduce the number of spokes from 21 to 13, and then reduce to 8 to observe the performance of the algorithm at a high acceleration factor. We compare the output images of the proposed algorithm with both the GRASP and NUFFT algorithms. In all the three modes (21, 13, and 8 spokes), the average image similarity is increased by at least by 0.4, 0.1 compared to NUFFT and GRASP, respectively. Moreover, the streaking artifacts are significantly reduced. According to the results obtained, the proposed method can be used on a clinical study for a fast dynamic MRI such as cardiac imaging with a high image quality from low- rate sampling.

Abbreviations	
MRI	Magnetic Resonance Imaging
GRASP	Golden Angle Radial Sparse Parallel MRI
FFT	Fast Fourier Transform
NUFFT	Non-Uniform Fast Fourier Transform
ASOS	Align Stack Of Stars
TV	Total Variation
CS	Compressive sensing
PSF	Point Spread Function
PI	Parallel Imaging
SENSE	Sensitivity Encoding

GRAPPA	GeneRalized Autocalibrating Partial Parallel Acquisition
DWT	Discrete Wavelet Transform
DCT	Discrete Cosine Transform
SSIM	Structural Similarity Index

1. Introduction

The limited imaging speed of MRI is a severe challenge in medical applications. In the late 1990s, a series of reconstruction techniques called Parallel

Imaging (PI) on MRI was introduced in order to accelerate the data acquisition process. In PI, several coils with different spatial sensitivities are used to perform part of the phase encoding process and utilize different algorithms like SENSE and GRAPPA in order to reconstruct the non-artifact images from an under-sampled k-space [1-4]. The advent of PI led to significant advances in MRI like the development of several rapid imaging techniques such as temporal parallel imaging and spatiotemporal acceleration techniques, often known as the k-t imaging techniques [5,6]. Another technique to address the unacceptable image quality and aliasing artifacts from sub-sampling is Compressive Sensing (CS). The concept of CS was first introduced in 2006 by Donoho and Candes et al. [7], and was soon translated to MRI by Lusting [8], which became a powerful approach to increase the imaging speed in MRI. CS took advantage of the fact that the images usually have a sparse representation; thus if the data is obtained incoherently, the image can be reconstructed using a small number of k-space data. CS-MRI has begun extensive research works in a variety of clinical fields including cardiovascular, body, neurological, and spectral imaging. Moreover, it has been shown that the combination of CS and PI will further increase the imaging speed beyond what is possible with only one method [9,10].

Non-Cartesian sampling such as a radial or spiral acquisition are other approaches for fast imaging. In radial sampling, k-space is not acquired directly on a uniform grid. Therefore, even the regular sampling of radial sampling results in an inherent incoherency. Moreover, due to the continuous update of the center of k-space in the radial acquisition, it is less sensitive to the respiratory motion, and therefore, the patient movement and breathing information can be obtained. However, the disadvantage of radial sampling is its reconstruction algorithm that is more complicated and time-consuming. In contrast, Cartesian sampling k-space is acquired on a uniform grid, and the image reconstruction is quick and effective due to FFT. Although the reconstruction of Cartesian data is computationally optimized and has a higher efficacy, there is a long history of non-Cartesian sampling since the beginning of MRI. In the recent years, this method has been widely used due to its higher acquisition speed and resistance to movement [6]. In particular, golden ratio radial sampling significantly improves the temporal

resolution. Golden angle radial sampling was first introduced for MRI in 2004 [11]. In this method, the angles of consecutive spokes are increased with a constant step of 111.25 degrees. This angle corresponds to the golden ratio ($g = (1+\sqrt{5})/2$), and makes any measurement of the data a complement to the previous coverage of the k-space, and the measurements never repeat. This acquisition scheme provides approximately a uniform coverage of the k-space for any arbitrary number of spokes, in particular, if its number belongs to the Fibonacci series [12]. It can also be extended to 3D Stack of Stars (SOS) by repeating the 2D data acquisition process for each slide [13]. The SOS method is widely used for dynamic imaging or motion-sensitive imaging such as angiography, cardiac imaging, and abdomen imaging [14].

In SOS volumetric imaging, the radial sampling is combined with Cartesian sampling with a hybrid sampling scheme such that the radial sampling is performed on the kx-ky plane and Cartesian sampling along kz. In the golden SOS sampling, instead of the linear step, a golden ratio is used as the angle between the adjacent spokes; the process is shown in Figure 1 [15]. Since the k-space is aligned through the kz, a 1D inverse Fourier transform (IFFT) is applied as an initial processing step, and enables a slide-by-slide reconstruction [12,15]. This procedure reduces the computational cost and allows for a direct reconstruction.

Image reconstruction with Total Variation (TV) has been the focus of the researchers for many years. This method will greatly help reduce the noise level in the images [16,17]. Compressibility of the image in both the TV field and the sparse space can be a prerequisite for producing a low noise level image [8,18]. In 2010, Otazu et al. obtained a significant acceleration rate by combining CS and PI at the k-t SPARSE-SENSE technique for dynamic MRI with Cartesian data [10]. In [19], the authors developed an accelerated 3D late gadolinium enhancement (LGE) pulse sequence using balanced steady-state free precession readout with stack-of-stars k-space sampling and extra motion-state golden-angle radial sparse parallel (XD-GRASP) reconstruction, and tested the performance for detecting atrial scar and fibrosis in the patients with atrial fibrillation (AF). In [20], Zhang et al. developed and evaluated an accelerated 3D self-gated cardiac cine imaging technique at 3 Tesla without the use of external electrocardiogram triggering or respiratory gating. In [21], the authors demonstrated the basic

functionality of SSA-FARY using numerical simulations, and applied it to in-vivo cardiac radial single-slice bSSFP and simultaneous multi-slice radiofrequency-spoiled gradient-echo measurements as well as Stack-of-Stars bSSFP measurements. In 2014, Li Feng et al. introduced the GRASP algorithm [15], and the idea of k-t SPARSE-SENSE [5] was extended for a volumetrically SOS data acquisition with a golden angle order acquisition. In the GRASP algorithm, a finite-difference of time frames is used as the sparse space. In other words, sparsity in the GRASP algorithm is in the time domain. This approach enables utilizing redundant information in time very well. Our goal in this work is to present a new formulation based on the combination of the GRASP method and the TV algorithm in order to produce a lower noise level image in the 4D data from the heart. Thus, at first, the basic concepts of CS and GRASP would be explained, and then the proposed algorithm will be discussed.

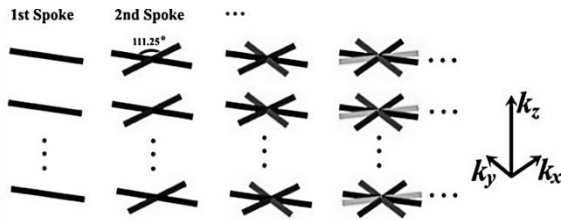


Figure. 1. Continues acquisition of radial spokes with 3D golden angle ASOS [16].

2. A Brief Overview of Compressive Sensing

The Nyquist theorem is a prerequisite for a correct signal reconstruction. Unfortunately, the Nyquist theorem requirement is often time-consuming and requires a large amount of memory for data transfer and storage in the design of sampling systems [12,22]. CS uses the sparsity to reconstruct signals from the samples less than the Nyquist rate instead of using the bandwidth limitation, and therefore, in this way, it can reduce the scan time significantly. However, the main problem of this theory is finding the solution of an underdetermined system of equations; the formulation is based on Equation 1 [22].

$$Y = \Phi S \quad (1)$$

where Φ is the sampling matrix or the coefficients matrix, and S is the sparse signal. This equation is more precisely expressed in the following equation:

$$y = \varphi s = \varphi \psi x = \theta x$$

$$.s = \sum_{i=1}^n x_i \psi_i \quad (2)$$

$$.s = \psi x$$

Where $\psi = [\psi_1 \psi_2 \psi_3 \dots \psi_N]$ is the sparsifying matrix and $X = [x_1 x_2 x_3 \dots x_n]$ is the coefficients vector. In this case, the number of equations is less than the number of unknowns. Therefore, it is underdetermined, and has numerous solutions. Thus in order to solve it and find a unique solution, we have to apply other conditions to the unknown vector. CS uses the sparsity to find the unique solution of the system. The general approach to solve it is given by Equation 3.

$$\min_s P_s P_0 \text{ Subject to } Y = \Phi S \quad (3)$$

The main idea of this method is to choose the sparsest vector among all the vectors in the above equation. Since the use of l0 norm leads to an NP-hard and non-convex problem, the only solution is an exhaustive search, which has a high computational cost and is not a practical approach. There are several methods for the reconstruction of sparse signals. The most common method is to approximate the cost function with a convex formulation, and then minimize it with convex optimization algorithms that provides an excellent signal reconstruction. The reason for the popularity of this method is the main theorem of convex optimization. According to this theorem, the local extremum of the problem also will be global extremum, which guarantees that we will converge to the correct answer [23]. There are three basic requirements for using CS [6]:

1. The sparsity or sparse representation of the target.
2. Incoherent sampling (incoherency between sampling and sparse domain).
3. Non-linear reconstruction algorithm that enforces sparsity with data consistency.

In what follows, each one of these three requirements will be explained [5].

2.1. Sparsity

If an image has only a small number of non-zero coefficients compared to the total number of voxels, it is sparse. An example of this is the MR angiography image, which suppresses the

background tissue area, and only the vessels represent the signal. Therefore, MR angiography is sparse in the image domain, which is not valid for all MRI images. However, a transformation such as DWT, DCT, and FFT is usually found that provides a sparse representation of the image. The number of measurements that are used to show the information directly related to the acceleration factor. A higher degree of sparsity is obtained during multi-dimensional processing like dynamic 3D imaging because the time dimension is highly compressible, and leads to a faster dynamic imaging than static imaging [6].

2.2. Incoherency

The second requirement for CS is that the artifacts from the sub-sampling should be incoherent; in other words, it should emerge as a noise-like pattern in the sparse space. This criterion is in contrast with regular sampling in Cartesian acquisition because, in this case, under-sampling leads to the correlated artifact in the images. The most popular solution is random under-sampling for Cartesian k-space, in which some steps of the phase encoding are eliminated randomly. Radial sampling is an attractive alternative due to its inherent incoherency behavior. The under-sampling artifacts in the radial acquisition, even with regular sampling, have higher incoherency than the Cartesian data. It also has other benefits such as high resistance to motion and breathing artifacts, which are particularly important in some imaging applications such as cardiac imaging. However, finding the optimal reconstruction algorithm for non-Cartesian data is still a major challenge.

2.3. Non-Linear Reconstruction Algorithm

CS reconstruction requires a problem that enforces the incoherence artifacts from the Nyquist sub-sampling, and maximizes the data consistency between the solution and the sub-sampled k-space data that is available. Finally, the problem can be mathematically formulated in Equation 4 [22].

$$\arg \min_m \|Tm\|_1 \quad \text{s.t.} \quad \|y - Fm\| < \varepsilon \quad (4)$$

where m is the reconstructed images, F is the Fourier transform corresponding to the data acquisition that maps the space between k-space

and image, y is the k-space (raw data), T is the sparsifying transform, and ε is the estimated noise level. The data consistency is checked by the l_2 norm, which determines the magnitude of the error between the measurements and the estimated data. The sparsity of the signal is controlled by minimizing the l_1 . Equation 4 tries to find the sparsest answer between all the solutions that have a lower error level than the error threshold. The l_1 minimization is widely used in the sparse reconstruction because a convex optimization problem will be obtained. The constrained optimization problem in Equation 5 can be rewritten in an unconstrained form with the help of Lagrange coefficients:

$$\arg \min_m Py - F_m P_2^2 + \lambda PT_m P_1 \quad (5)$$

The optimization problem in (5) can be solved using the iterative algorithms such as the descending gradient method or other convex problem-solving algorithms. These algorithms start by reducing the number of artifacts at each iteration. The coefficient λ also has the function of controlling the data consistency (12) and sparsity (11) [6,15,24]. A TV penalty is usually used to reduce noise levels. The formulation will be as follows:

$$\arg \min_m \|y - Fm\|_2^2 + \lambda \|Tm\|_1 + \beta TV(m) \quad (6)$$

where β controls the sparse representation coefficients with the TV-coefficient, and λ , F , T , m , and y are the same in Equation 6.

3. GRASP Formulation

The formulation of the GRASP method is according to Equation 7 [15].

$$\hat{d} = \arg \min \|FSd - m\|_2^2 + \lambda \|Td\|_1 \quad (7)$$

where d is the reconstructed images set, T is the temporal total variation imposed on the l_1 norm, $m = [m_1 m_2 \dots m_c]$ is the radial k-space data of all coils (assuming the number of coils is c), F is the NUFFT [25], $S = [s_1 s_2 \dots s_c]$ is the coil sensitivity matrix, and λ is the parameter for balancing the sparsity and the data consistency in CS. In this work, the idea of the GRASP method is combined with the total variation denoising

algorithm, and results are compared with the GRASP and NUFFT reconstructions.

4. Method

TV on the third constraint is the difference between the adjacent pixels on each image that controls the noise, β is a weighting parameter to control the sparsity from sparsifying transform and TV sparsity of each individual image, And F , S , d , m , λ , and T are the same as the Equation 7. In order to determine the optimal value of λ , the performance of several different values of λ on a dataset with a specified time resolution (21, 13, and 8 spokes per time frame) was evaluated. The reconstructions were performed using weights ranging from $0.01 * I_0$ to $0.1 * I_0$ (step size 0.01), where I_0 is the maximum value in the NUFFT images used to initialize the iterative method. Finally, $0.025 * I_0$ for the λ parameter and $0.1 * I_0$ for the β parameter were considered as the final values. According to the Nyquist rate, the number of samples required in this case is $384 * 2 / \pi = 604$, which will result in the acceleration factor of 28.7, 46.4, and 75.5 (21 spokes: $604/21 = 28.7$, 13 spokes: $604/13 = 46.4$ and 8 spokes: $604/8 = 75.5$). The Point Spread Function (PSF) indicates the degree of incoherency associated with the radial sub-sampling before applying CS. In order to calculate PSF, we consider the value of the raw data one, and then apply the NUFFT to reconstruct the images. Based on the results obtained, the lateral edges will decrease in the 21 spokes to 1_3 and 8 spokes.

5. Results

The data used in this work is a cardiac image series with dimensions of $256 * 256 * 20 * 11$ (20 temporal frames, 11 slices, and $256 * 256 = X * Y$) [26]. These images are first interpolated into the Cartesian k-space data and then into the radial data (3D SOS with golden ratio step). The dimensions of the initial k-space are $600 * 768$ ($K_x * K_y$) for each slice. PSF in this algorithm was determined for three cases (21, 13, and 8 spokes) and was depicted in two angles of view, from above and from the side, as shown in Figure 2. The degree of correlation was calculated by the ratio of the main

lobe to the side lobe. The values for the 8th, 13th, and 21st spokes are 30.09, 32.16, and 34.27, respectively, which verify the improvement of incoherency.

The reconstructed images are aimed for quantification of the myocardium, which is located in the central part of the image. Therefore, for each reconstruction, the structural similarity index (denoted as SSIM) in the central part of the image (a box with a $96 * 96$ pixel area) was measured in comparison with the original images to quantify the visual difference from the original image. Since the key point in the cardiac imaging assessment is the structure of anatomy (cardiac), the coefficients of 1 and 0.75 were considered for the structure and contrast, and 0 for the illumination in SSIM. The SSIM values for the reconstructed images using the proposed method on the under-sampled data were calculated and compared to SSIM of the images reconstructed by NUFFT and GRASP (reported in Table 1). The average quality improvement of all images was near 0.1 in comparison to GRASP. The images reconstructed with NUFFT and the proposed algorithm are shown in Figure 3, and the reference images in Figure 4. Clearly, the artifacts significantly decreased in images processed by the proposed method. According to Figure 3, as well as similarity index in Table 1, the images reconstructed with the proposed algorithm in this work have the most considerable similarity to the reference images. Due to a large number of images and the slide-by-slide reconstruction, only the images belonging to the 1st, 8th, 14th, and 20th temporal frames of the 2nd, 4th, 6th, and 10th slices were presented. In all reconstructions, the values of λ and β are 0.025, and 0.1 maximum of the initial image reconstructed with NUFFT, respectively. According to the last column in Table 1 (averaged through the partitions), the similarity increased more than 0.4, 0.48, and 0.54 for 21st, 13th, and 8th spokes, respectively, over the NUFFT through the whole volume. All three groups also improved on average by at least 0.1 compared to GRASP, while the required time and computation cost did not increase.

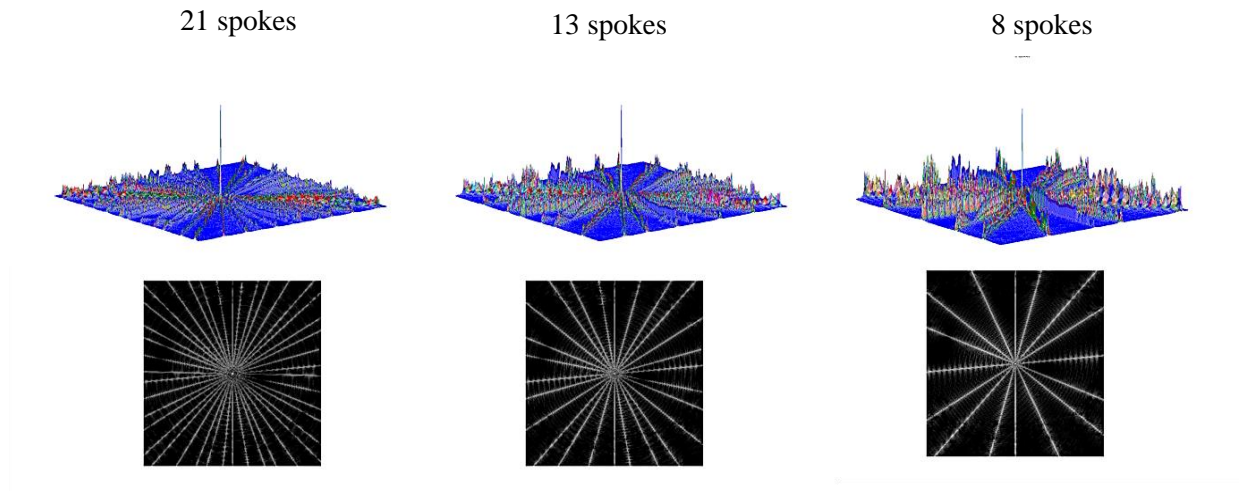


Figure 2. Point spread function (PSF) of an undersampled radial trajectories, 21, 13 and 8 golden angle spokes in 3D Align Stack of Stars (ASOS).

Table 1. Image quality assessment scores represent SSIM for each reconstruction category (21, 13 and 8 spokes with NUFFT, GRASP and proposed method), The bold numbers are the maximum value of each method.

Slice Number	1	2	3	4	5	6	7	8	9	10	11	Ave	Spokes Number
GRASP	0.85	0.84	0.83	0.82	0.83	0.81	0.82	0.80	0.78	0.73	0.72	0.80	21
NUFFT	0.50	0.49	0.51	0.48	0.49	0.47	0.51	0.51	0.52	0.49	0.50	0.49	
Proposed Method	0.86	0.87	0.88	0.89	0.89	0.89	0.90	0.89	0.90	0.91	0.92	0.89	
GRASP	0.78	0.78	0.77	0.77	0.77	0.74	0.75	0.76	0.74	0.72	0.71	0.75	13
NUFFT	0.36	0.35	0.38	0.37	0.36	0.35	0.39	0.39	0.39	0.36	0.39	0.37	
Proposed Method	0.82	0.83	0.84	0.84	0.85	0.86	0.88	0.87	0.86	0.85	0.86	0.85	
GRASP	0.70	0.72	0.69	0.74	0.73	0.75	0.75	0.70	0.77	0.72	0.70	0.72	8
NUFFT	0.26	0.25	0.27	0.27	0.27	0.26	0.28	0.29	0.29	0.27	0.28	0.27	
Proposed Method	0.81	0.81	0.82	0.83	0.84	0.82	0.83	0.81	0.82	0.80	0.79	0.81	

6. Discussion

The main difficulty of all the iterative algorithms is their speed and computational cost. Both the GRASP and proposed methods are time-consuming due to the interpolation steps of NUFFT at each iteration so the elimination of the interpolation steps may solve this drawback.

Recently Polar Fourier Transform (PFT) [27] has been introduced by Golshani et al., which can reconstruct the radial data without any interpolation steps; thus PFT can be an alternative for NUFFT. By using PFT instead of NUFFT in the proposed method, the time-consuming issue probably would be solved.

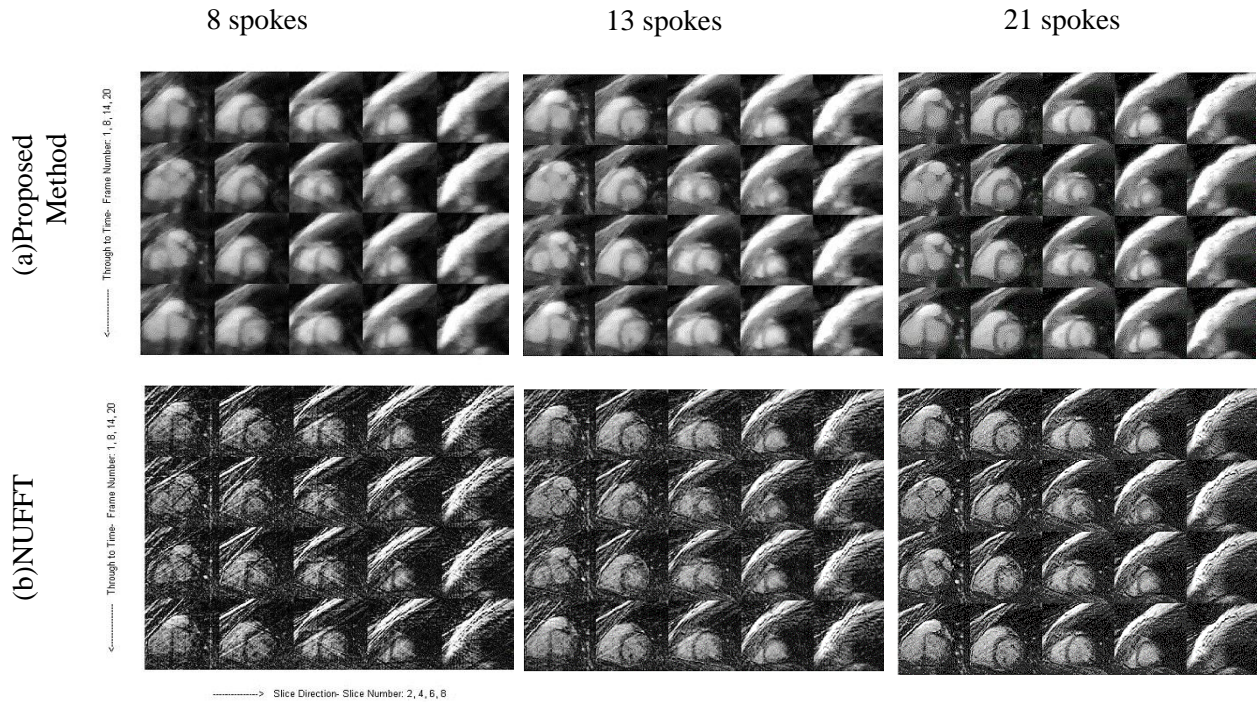


Figure. 3. Reconstruction of five representative partition from the simulation golden-angle volumetric cardiac dataset using (a) proposed method (b)NUFFT with three different spokes number: 21, 13 and 8.

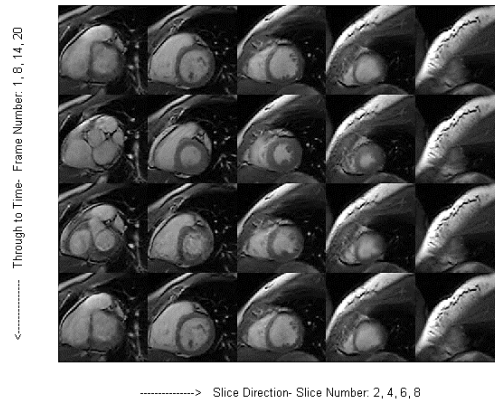


Figure. 4. Original Images (Ground truth).

7. Conclusion

In this work, we proposed a reconstruction method based on a combination of the TV and GRASP methods for highly under-sampled ASOS-golden angle cardiac MRI data, and calculated PSF in order to investigate the degree of incoherency. In the images reconstructed by the proposed method, the streaking artifact significantly declined. The similarity between the sub-sampled (only 8 spokes)

and reference images enhanced more than 0.81, while the time complexity and computational cost were almost the same with the GRASP algorithm and did not increase. By reducing the number of spokes from 21 to 8, the resistance of the proposed algorithm to different sampling rates was also investigated. Even the visual comparison of the results proves the improvement of the image quality using the proposed method. In brief, in this work,

three approaches were compared with each other, and finally, high-resolution images were successfully reconstructed at a high acceleration rate by the proposed method.

Acknowledgment

This work was supported by Babol Noshirvani University of Technology research grant # BNUT P/M/1103.

References

- [1] D. C Peters, P. Rohatgi, R. M. Botnar, S. B. Yeon, K. V. Kissinger, and W. J. Manning, "Characterizing radial undersampling artifacts for cardiac applications." *Magnetic Resonance in Medicine*, vol. 55, no. 2, pp. 396-403, 2006.
- [2] D. K. Sodickson, and C. A. McKenzie, "A generalized approach to parallel magnetic resonance imaging." *Medical physics*, vol. 28, no. 8, pp. 1629-1643, 2001.
- [3] K. P. Pruessmann, M. Weiger, M. B. Scheidegger, and P. Boesiger, "SENSE: sensitivity encoding for fast MRI." *Magnetic Resonance in Medicine*, vol. 42, no. 5, pp. 952-962, 1999.
- [4] M. A. Griswold, P. M. Jakob, R. M. Heidemann, M. Nittka, V. Jellus, J. Wang, B. Kiefer, and A. Haase, "Generalized autocalibrating partially parallel acquisitions (GRAPPA)," *Magnetic Resonance in Medicine*, vol. 47, no. 6, pp. 1202-1210, 2002.
- [5] M. Lustig, J. M. Santos, D. L. Donoho, and J. M. Pauly. "k-t SPARSE: High frame rate dynamic MRI exploiting spatio-temporal sparsity." *Proceedings of the 13th annual meeting of ISMRM, Seattle*. 2006.
- [6] L. Feng, T. Benkert, K. T. Block, D. K. Sodickson, R. Otazo, and H. Chandarana, "Compressed sensing for body MRI," *Journal of Magnetic Resonance Imaging*, vol. 45, no. 4, pp. 966-987, 2017.
- [7] E. J. Candès, "Compressive sampling." in *Proceedings of the international congress of mathematicians*. Madrid, Spain, 2006.
- [8] M. Lustig, D. Donoho, and J. M. Pauly, "Sparse MRI: The application of compressed sensing for rapid MR imaging". *Magnetic Resonance in Medicine*, vol. 58, no. 6, pp. 1182-1195, 2007.
- [9] K. T. Block, M. Uecker, and J. Frahm, "Undersampled radial MRI with multiple coils. Iterative image reconstruction using a total variation constraint." *Magnetic Resonance in Medicine*, vol. 57, no. 6, pp. 1086-1098, 2007.
- [10] R. Otazo, D. Kim, L. Axel, and D. K. Sodickson, "Combination of compressed sensing and parallel imaging for highly accelerated firstpass cardiac perfusion MRI," *Magnetic resonance in medicine*, vol. 64, no. 3, pp. 767-776, 2010.
- [11] T. Kohler, "A projection access scheme for iterative reconstruction based on the golden section." in *IEEE Symposium Conference Record Nuclear Science*, vol. 6, pp. 3961-3965, 2004.
- [12] K. T. Block, H. Chandarana, S. Milla, M. Bruno, T. Mulholland, G. Fatterpekar, M. Hagiwara, R. Grimm, C. Geppert, B. Kiefer, and D. K. Sodickson, "Towards routine clinical use of radial stack-of-stars 3D gradient-echo sequences for reducing motion sensitivity". *Journal of the Korean Society of Magnetic Resonance in Medicine*, vol. 18, no. 2, pp. 87-106, 2014.
- [13] L. Feng, R. Grimm, K. T. Block, H. Chandarana, S. Kim, J. Xu, L. Axel, D. K. Sodickson, and R. Otazo, "High spatial and temporal resolution 2D real time and 3D whole-heart cardiac cine MRI using compressed sensing and parallel imaging with golden angle radial trajectory." in *Proceedings of the 20th Annual Meeting of ISMRM, Melbourne, Australia*. 2012.
- [14] O. Sayin, H. Saybasili, M. M. Zviman, M. Griswold, H. Halperin, N. Seiberlich, and D. A. Herzka, "Real-time free-breathing cardiac imaging with self-calibrated through-time radial GRAPPA." *Magnetic resonance in medicine*, vol. 77, no. 1, pp. 250-264, 2017.
- [15] L. Feng, R. Grimm, K. T. Block, H. Chandarana, S. Kim, J. Xu, L. Axel, D. K. Sodickson, and R. Otazo, "Golden-angle radial sparse parallel MRI: combination of compressed sensing, parallel imaging, and golden-angle radial sampling for fast and flexible dynamic volumetric MRI." *Magnetic resonance in medicine*, vol. 72, no. 3, pp. 707-717, 2014.
- [16] L.I. Rudin, S. Osher, and E. Fatemi, "Non-linear total variation based noise removal algorithms." *Physica D: nonlinear phenomena*, vol. 60, no. (1-4) , pp. 259-268, 1992.
- [17] E. Sahragard, H. Farsi, S. Mohammadzadeh, "Image Restoration by Variable Splitting based on Total Variant Regularizer." *Journal of AI and Data Mining*, vol. 6, no. 1, pp. 13-33, 2018.
- [18] Y. Tsaig, and D.L. Donoho, "Extensions of compressed sensing." *Signal processing*, vol. 86, no. 3, pp. 549-571, 2006.
- [19] S. Gunasekaran, H. Haji-Valizadeh, D. C. Lee, R. J. Avery, B. D. Wilson, M. Ibrahim, M. Markl, R. S. Passman, E. G. Kholmovski, and D. Kim. "Accelerated 3D Left Atrial Late Gadolinium Enhancement in Patients with Atrial Fibrillation at 1.5 T: Technical Development," *Radiology: Cardiothoracic Imaging*, vol. 2, no. 5, 2020.

- [20] X. Zhang, G. Xie, N. Lu, Y. Zhu, Z. Wei, S. Su, C. Shi, F. Yan, X. Liu, B. Qiu, and Z. Fan. "3D self-gated cardiac cine imaging at 3 Tesla using stack-of-stars bSSFP with tiny golden angles and compressed sensing," *Magn Reson Med*. vol. 81, no. 5, pp. 3234-3244, 2019.
- [21] S. Rosenzweig, N. Scholand, H. C. M. Holme, and M. Uecker. "Cardiac and Respiratory Self-Gating in Radial MRI Using an Adapted Singular Spectrum Analysis (SSA-FARY)," *IEEE Trans Med Imaging*, vol. 39, no. 10, pp. 3029-3041, 2020.
- [22] M. Lustig, D. L. Donoho, J. M. Santos, and J. M. Pauly, "Compressed sensing MRI." *IEEE signal processing magazine*, vol. 25, no. 2, pp. 72-82, 2008.
- [23] Z. Q. Luo, and W. Yu, "An introduction to convex optimization for communications and signal processing." *IEEE Journal on selected areas in communications*, vol. 24, no. 8, pp. 1426-1438, 2006.
- [24] L. Feng, L. Axel, H. Chandarana, K. T. Block, D. K. Sodickson, and R. Otazo, "XD-GRASP: golden-angle radial MRI with reconstruction of extra motion-state dimensions using compressed sensing." *Magnetic resonance in medicine*, vol. 75, no. 2, pp. 775-788, 2016.
- [25] J. A. Fessler, and B. P. Sutton. "Non-uniform fast Fourier transforms using min-max interpolation." *IEEE transactions on signal processing*, vol. 51, no. 2, pp. 560-574, 2003.
- [26] A. Andeopoulos, and J. K. Tsotsos, *Efficient and generalizable statistical models of shape and appearance for analysis of cardiac MRI*. Medical Image Analysis, vol. 12, no. 3, pp. 335-357, 2008.
- [27] S. Golshani, and A. Nasiraei-Moghaddam. "Efficient radial tagging CMR exam: A coherent k-space reading and image reconstruction approach." *Magnetic resonance in medicine*, vol. 77, no. 4, pp. 1459-1472, 2017.

بازسازی داده سه بعدی Stack of Stars در تصویربرداری تشدید مغناطیسی با استفاده از ادغام روش- های TV و GRASP

میترا توکلی^۱، عطاالله ابراهیم زاده^۱، عباس نصیرایی مقدم^۲ و جواد کاظمی تبار^{۱*}

^۱دانشکده مهندسی برق و کامپیوتر، دانشگاه صنعتی نوشیروانی بابل، مازندران، ایران.

^۲دانشکده مهندسی پزشکی، دانشگاه صنعتی امیرکبیر، تهران، ایران.

ارسال ۲۰۲۰/۱۱/۰۶؛ بازنگری ۲۰۲۱/۰۶/۲۵؛ پذیرش ۲۰۲۱/۰۹/۰۵

چکیده:

یکی از پیشرفته‌ترین روشهای تصویربرداری غیرتهاجمی، تصویربرداری تشدید مغناطیسی است که می‌تواند تضاد خوبی بین بافتهای نرم ایجاد کند. هرچند مشکل اصلی این روش محدودیت زمانی در اخذ داده، به ویژه در تصویربرداری پویا است. از روشهای پرکاربرد برای افزایش سرعت اخذ داده در تصویربرداری تشدید مغناطیسی می‌توان به نمونه‌برداری شعاعی اشاره کرد. این روش مزایای متعددی را در مقایسه با نمونه‌برداری کارت‌تیزین دارد. از جمله آنها مقاومت در برابر آرتیفکتهای حرکتی می‌باشد. در سالهای اخیر از سنجش فشرده نیز برای سرعت بخشیدن به گرفتن اطلاعات در تصویربرداری تشدید مغناطیسی استفاده شده است. برای استفاده از این روش، نیاز به وجود آرتیفکتهای ناهمبسته است که از طریق نمونه برداری نامنظم در اخذ کارت‌تیزین، قابل دستیابی است. این الزام در اخذ شعاعی بخاطر آرتیفکتهای ناهمبسته‌ای که حتی با طرحهای منظم نمونه‌برداری، ایجاد می‌کند؛ به خوبی برآورده می‌شود. در این پژوهش به بازسازی داده سه بعدی در تصویربرداری قلب با استفاده از اضافه کردن یک تابع جریمه مربوط به تغییرات کلی هر تصویر-Total-Variation- در فرمول‌بندی روش اخذ و بازسازی GRASP در حالت ۲۱ اسپوک پرداختیم. مقایسه تصاویر خروجی با هر دو الگوریتم GRASP و تبدیل فوریه غیریکنواخت نشان داد که میزان شباهت تصاویر ۰.۳۹ نسبت به تبدیل فوریه غیریکنواخت افزایش داشته است. کاهش چشمگیر آرتیفکتهای خط خط در هر سه حالت بصورت بصری نیز واضح می‌باشد. بنابر یافته‌های این مقاله روش پیشنهادی می‌تواند برای افزایش سرعت تصویربرداری تشدید مغناطیسی پویا برای ساخت تصاویر با کیفیت بالا در نمونه‌برداری زیرنرخ نایکوئیست استفاده شود.

کلمات کلیدی: تصویر برداری تشدید مغناطیسی قلب، اخذ شعاعی با زاویه طلایی، حسگری فشرده.